Laser and Particle Beams (2013), *31*, 387–394.

doi:10.1017/S0263034613000384

Stimulated Raman backscattering of filamented hollow Gaussian beams

RAM KISHOR SINGH AND R.P. SHARMA
Centre for Energy Studies, Delhi, India
(RECEIVED 26 January 2013; ACCEPTED 7 April 2013)

Abstract

This paper presents a model for excitation of electron plasma wave and resulting stimulated Raman scattering due to presence of a laser beam carrying null intensity in center (hollow Gaussian beam) in a collisionless plasma. We have studied the self-focusing of the hollow Gaussian beam and its effect on back stimulated Raman scattering process in the presence of ponderomotive nonlinearity. To understand the nature of propagation of the hollow Gaussian beam, electron plasma wave and back reflectivity, a paraxial-ray approximation has been invoked. It is predicted that self-focusing and back reflectivity reduces for higher order of hollow Gaussian beam.

Keywords: Electron plasma wave; Hollow Gaussian Laser beam; Ponderomotive nonlinearity; Self-focusing; Stimulated Raman scattering

1. INTRODUCTION

The interaction of high irradiance electromagnetic beams with homogeneous plasma is a topic of extensive research in many areas like optical harmonic generation (Sprangle *et al.*, 1991; Milchberg *et al.*, 1995), laser-induced fusion (Tabak *et al.*, 1994; Kruer, 1974), and laser-driven accelerators (Sprangle *et al.*, 1988; Umstadter *et al.*, 1996). Self-focusing of a laser beam and back stimulated Raman scattering are very important nonlinear processes in laser induced fusion and it has been investigated experimentally (Kirkwood *et al.*, 2006; Tajima *et al.*, 1979) and theoretically (Akhmanov *et al.*, 1968; Umstadter *et al.*, 1996; 1997). Self-focused laser beam may produce energetic electrons (Kaw *et al.*, 1973), which may preheat the fusion fuel and affect the compression while the energy associated with back scattered wave is wasted. Various spatial profile of laser beam has been used to study the laser plasma interaction, like as; Gaussian beam (Akhmanov *et al.*, 1968), super Gaussian beam (Grow *et al.*, 2006), dark hollow Gaussian beam (DHBs) (Sodha *et al.*, 2009). A collimated laser beam can be described by Laguerre-Gaussian functions, which provides a natural orthonormal basis (Allen *et al.*, 1992). Laguerre-Gaussian mode well defined by L_p^1, or specifically L_m^{n-m} (r^2) where p and $(l = n - m)$ are associated with radial index and azimuthal index mode respectively (see Section 2). The amplitude of a Laguerre-Gaussian mode has an azimuthal angular dependence of $\exp(il\theta)$ (Allen *et al.*, 1992). For $p = 0$ and $l \geq 1$, the intensity of the laser beams have ring like structure and the associated magnitude of the amplitude part of the laser beam can be described by hollow Gaussian function. Hollow Gaussian beams (HGBs) can be expressed as a superposition of a series of Lagurerre-Gaussian modes (Cai *et al.*, 2003). An optical beam with null intensity at center is called dark hollow laser beam (DHB); the best-known example is a $TEM_{01}{}^*$ beam. Various methods have been developed for creating dark spot laser beams, like the holographic method (Lee *et al.*, 1994), the geometrical optical method (Herman *et al.*, 1991), transverse mode selection method (Wang *et al.*, 1993), and a conical lens (Song *et al.*, 1999). The propagation dynamics of the beam is sensitive to transverse profile of the beam and propagation of HGBs through paraxial optical system have been described for the free space (Cai *et al.*, 2003; 2004), in a turbulent atmosphere (Cai *et al.*, 2006) and homogeneous non-magnetized plasma (Sodha *et al.*, 2009). The self-focusing of HGBs (Sodha *et al.*, 2009; Gill *et al.*, 2010) and cross focusing of HGBs (Gupta *et al.*, 2011) has been investigated theoretically in plasmas.

The growth of SRS has been investigated experimentally (Fuchs *et al.*, 2000) in a variety of conditions, including laser smoothing and focusing conditions, varying laser

Address correspondence and reprint requests to: Ram Kishor Singh, Centre for Energy Studies, IIT Delhi, India 110016. E-mail: ram007kishor@gmail.com

intensities and plasma densities. The SRS process gets affected due to the self-focusing and filamentation of the pump beam. The filament formation and its effects on SRS have been observed by using the PIC simulations (Matsuoka *et al.*, 2008). The past experimental results on SRS process did not match with the theoretical results. In the theoretical models, the beams have Gaussian profile with TEM_{00} mode and the wave equations have been solved in either paraxial or extended paraxial regime, but in many experimental situation the pump beams are the superposition of higher order modes. For the deep understanding of SRS process, the theoretical analysis is needed for the higher order mode of the waves.

In this work, we have theoretically investigated excitation of electron plasma wave, stimulated Raman scattering for the different orders of self-focused HGBs in collisionless plasma, considering ponderomotive nonlinearity, using paraxial approximation. When pump beam, having frequency ω_0 and wave number $\vec{k}_0$, interacts with pre-excited electron plasma wave, having frequency ω and wave number $\vec{k}$, generates scattered beam, known as stimulated Raman scattered (SRS) wave, of frequency $(\omega_0 - \omega)$ and wave number $\left(\vec{k}_0 - \vec{k}\right)$.

This article is organized as follows: In Section 2, we have given the expression for the beam width parameter of the HGBs and equations for the excitation of the electron plasma wave when ponderomotive nonlinearity is taken in to account. In Section 3, the basic equations that govern the dynamics of SRS process and back SRS reflectivity of the beam, consider the paraxial approximation. In Section 4, we have discussed numerical results and the last section is devoted to the conclusions based on the present investigation.

2. PROPAGATION OF HOLLOW GAUSSIAN LASER BEAM AND EXCITATION OF ELECTRON PLASMA WAVE

When a high power laser beam (pump) of frequency ω_0 and wave vector $\vec{k}_0$ is propagating in collisionless and homogeneous plasma along the z direction, the transverse intensity gradient generates a ponderomotive force, which modifies the plasma density profile in the transverse direction. Due to this redistribution of carriers, a transverse gradient of effective dielectric constant is established which leads to self-focusing of the electromagnetic beam. The wave equation in isotropic and homogeneous plasma can be written as:

$$\nabla^2 E - \nabla(\nabla . E) + \frac{\varepsilon(r, z)\omega_0^2}{c^2}\frac{\partial^2 E}{\partial t^2} = 0. \tag{1}$$

For transverse field $\nabla(\nabla \cdot \mathrm{E}) = 0$, where the symbols have as usual meanings. The solution of Eq. (1) in cylindrical coordinates can be written as:

$$E(r, \theta, z) = E_0(r, \theta, z)e^{-i(k_0 z - \omega_0 t)}. \tag{2}$$

Where, $k_0 = \frac{\omega_0}{c}\sqrt{\varepsilon_0}$ is the wave vector and ω_0 is the frequency of the laser beam. In the case of linear approximation (weak laser power), Eq. (1) will reduce to pure paraxial equation and takes the form (Mendonca *et al.*, 2009),

$$\left(\nabla_\perp^2 + 2ik_0\frac{\partial}{\partial z}\right)E_0(r, \theta, z) = 0. \tag{3}$$

The paraxial wave solution of Eq. (3) can be written as linear combination of the modes $E_0(r,\theta,z) = E_{p,l}(z)F_{p,l}(r,z)e^{il\theta}$, where $F_{p,l}(r,z)$ is the Laguerre-Gaussian function, with integer p, l representing the radial and azimuthal number (Mendonca *et al.*, 2009). For $p = 0$ and $l = 0$, the laser beam has fundamental Gaussian TEM_{00} mode which has maximum intensity at the center but for $p = 0$ and $l \geq 1$, intensity is null at the center. The nonlinear dielectric constant $\varepsilon(r,z)$ is a function of intensity of the high power laser and the nonlinearity arises in plasma due to nonlinear dependence of the free carrier density on the electric field vector. In case of nonlinear medium (strong laser power), the propagation dynamics of Lagurerre-Gaussian beam is complicated because the phase front of the beam is rotating. For Simplicity, we have taken HGBs which have intensity null at the center and the initial field distribution of hollow Gaussian laser beam can be given by

$$(E)_{z=0} = E_0\left(\frac{r^2}{2r_0^2}\right)^n \exp\left(-\frac{r^2}{2r_0^2}\right). \tag{4}$$

Where, r_0 is the initial beam width, n is the order of the HGBs, and E_0 is the maximum amplitude of the laser beam around $r = r_{\max} = r_0\sqrt{2n}$. The modified electron density profile of the plasma due to ponderomotive force can be written as (Sodha *et al.*, 1976)

$$N_{0e} = N_0 \exp\left(-\frac{3}{4}\alpha\frac{m_e}{m_i}E.E^{\cdot}\right). \tag{5}$$

Where, $\alpha = e^2 m_e/6k_B T_0 \gamma m_e^2 \omega_0^2$ is nonlinearity parameter, N_0 is the density of plasma electrons in the absence of laser beam, k_B is the Boltzmann's constant, T_0 is the equilibrium plasma temperature and γ is the ratio of the specific heats.

Consider the solution of Eq. (1) is

$$E_0(r, z) = \hat{i}A(r, z)\exp(-ik_0 z), \tag{6}$$

Where $A(r,z)$ is the complex amplitude of the wave. From Eqs. (1) and (6) we get,

$$2ik\frac{\partial A}{\partial z} = \left(\frac{\partial^2 A}{\partial r^2} + \frac{1}{r}\frac{\partial A}{\partial r}\right) + \frac{\omega_0^2}{c^2}(\varepsilon - \varepsilon_0)A. \tag{7}$$

The complex amplitude $A(r,z)$ can be represented as

$$A(r, z) = A_0(r, z)\exp\left\{-ik_0 S_0(r, z)\right\}. \tag{8}$$

Now transform the (r, z) coordinate in to (η, z) coordinate as

$$\eta = \left(\frac{r}{r_0 f_0} - \sqrt{2n}\right). \tag{9}$$

Where, $r_0 f_0$ is the beam width of laser beam and maximum irradiance at $r = r_0 f_0\sqrt{2n}$. For paraxial ray approximation $\eta \ll \sqrt{2n}$ and A_0 is defined as

$$A_0^2 = \frac{E_0^2}{2^{2n} f_0^2}\left(\sqrt{2n} + \eta\right)^{4n}\exp\left\{-\left(\sqrt{2n} + \eta\right)^2\right\}, \tag{10}$$

and eikonal of the pump beam is given as

$$S_0(\eta, z) = \frac{\left(\sqrt{2n} + \eta\right)^2 r_0^2 f_0}{2}\frac{df_0}{dz} + \phi(z). \tag{11}$$

The dimensionless beam width parameter f_0 can be obtained by using the boundary conditions $f_0|_{z=0} = 1$ and $df_0/dz|_{z=0} = 0$ (Akhmanov *et al.*, 1968)

$$\varepsilon_0 f_0 \frac{d^2 f_0}{d\xi^2} = \frac{4}{f_0^2} - \varepsilon_2 \rho_0^2. \tag{12}$$

Where $\xi = \frac{c}{r_0^2\omega_0} z$ is dimensionless parameter and $\rho_0^2 = \frac{r_0^2\omega_0^2}{c^2}$. In the presence of ponderomotive force, the plasma density varies through the plasma channel and the dielectric function $\varepsilon(\eta, z)$ may be expressed as

$$\varepsilon(\eta, z) = 1 - \frac{\omega_p^2}{\omega_0^2}\exp\left\{-\frac{3}{4}\alpha\frac{m_e}{m_i}\frac{E_0^2}{f_0^2}\left(\frac{\left(\eta + \sqrt{2n}\right)^2}{2}\right)^{2n} \times \exp\left\{-\left(\eta + \sqrt{2n}\right)^2\right\}\right\}, \tag{13}$$

and

$$\varepsilon_0(z) = 1 - \frac{\omega_p^2}{\omega_0^2}\left\{\exp\left(-\frac{3}{4}\alpha\frac{m_e}{m_i}\frac{E_0^2}{f_0^2} n^{2n} e^{-2n}\right)\right\}, \tag{14}$$

$$\varepsilon_2(z) = 2\left(\frac{\omega_p^2}{\omega_0^2}\frac{3}{4}\alpha\frac{m_e}{m_i}\frac{E_0^2}{f_0^2} n^{2n} e^{-2n}\right)\exp\left(-\frac{3}{4}\alpha\frac{m_e}{m_i}\frac{E_0^2}{f_0^2} n^{2n} e^{-2n}\right). \tag{15}$$

Electron plasma wave (EPW) is excited in the presence of HGBs. For analysis of EPW in the presence of ponderomotive nonlinearity and filamented laser beam, the following equations are used.

The equation of motion can be written as

$$m_e\left[\frac{\partial V}{\partial t} + (V.\nabla)V\right] = -eE - \frac{e}{c}(V \times B) - 2\Gamma_e m_e V - \frac{\gamma k_B T_0}{N}\nabla N. \tag{16}$$

Where $\Gamma_e \approx \frac{1}{2}\sqrt{\frac{\pi}{8}}\frac{\omega_p}{k^3\lambda_d^3}\exp\left(-\frac{3}{2} - \frac{1}{2k^2\lambda_d^2}\right)$ is the Landau damping factor, V is the electron fluid velocity, N is the instantaneous electron density, E and B are associated with electric and magnetic field vectors, and $\lambda_d = \left(\frac{k_B T_0}{4\pi n_0 e^2}\right)^{\frac{1}{2}}$ is the Debye length and k is the wave vector of the electrostatic wave. The continuity equation can be written as

$$\frac{\partial N}{\partial t} + \nabla.(NV) = 0. \tag{17}$$

From the Poisson's equation, one can get

$$\nabla.E = -4\pi e N. \tag{18}$$

Applying the perturbation approximation,

$N = N_{0e} + n_{e0}$ and $V = V_0 + v$; where $n_{e0} \ll N_{0e}$ & $v \ll V_0$.

Solving Eqs. (16), (17), and (18), one obtains the general equation, which governs the electron density variation

$$\frac{\partial^2 n_{e0}}{\partial t^2} + 2\Gamma_e\frac{\partial n_{e0}}{\partial t} - \gamma v_{th}^2\nabla^2 n_{e0} + \omega_p^2\exp\left(-\frac{3}{4}\alpha\frac{m_e}{m_i}EE*\right)n_{e0} \simeq 0. \tag{19}$$

Where, v_{th} is the electron thermal speed. Consider a plane wave solution of Eq. (19),

$$n_{e0} = n_{e00}(r, z)\exp\left\{i(\omega t - kz - S(r, z))\right\}. \tag{20}$$

Where, ω and k are frequency and wave vector of the plasma wave and satisfy the Bohm-Gross dispersion relation

$$\omega^2 = \omega_p^2\frac{N_{0e}}{N_0} + \gamma k^2 v_{th}^2. \tag{21}$$

Using the value of n_{e0} from Eq. (20) into Eq. (21) and separating the real and imaginary part, one gets

$$2\frac{\partial S}{\partial z} + \left(\frac{\partial S}{\partial r}\right)^2 = \frac{1}{k^2 n_{e00}}\left[\frac{1}{r}\left(\frac{\partial n_{e00}}{\partial r}\right) + \frac{\partial^2 n_{e00}}{\partial r^2}\right] + \frac{\omega_p^2}{\gamma k^2 v_{th}^2}\left(1 - \frac{N_{0e}}{N_0}\right), \tag{22}$$

$$2\frac{\partial n_{e00}^2}{\partial z}+\frac{\partial S}{\partial r}\left(\frac{\partial n_{e00}^2}{\partial r}\right)+n_{e00}^2\frac{1}{k^2}\left[\frac{1}{r}\left(\frac{\partial S}{\partial r}\right)+\frac{\partial^2 S}{\partial r^2}\right]+\frac{2\Gamma_e}{3v_{th}^2}\frac{\omega n_{e00}^2}{k}=0. \quad (23)$$

Now transform the (r, z) coordinate in to (η, z) coordinate by using the Eq. (9). Hence Eqs. (22) and (23) can be solved in paraxial ray approximation and the solution is (for initial HGB distribution)

$$n_{e00}^2=\frac{N_{e00}^2}{f_e^2 2^{2n}}\left(\eta+\sqrt{2n}\right)^{4n}\left(\frac{r_0 f_0}{af_e}\right)^{4n}\exp\left(-\left(\eta+\sqrt{2n}\right)^2-2k_i z\right). \quad (24)$$

Where, f_e and a are the dimensionless beam width parameter and radius of EPW, respectively. The eikonal of the electron plasma wave is described by,

$$S=\left(\eta+\sqrt{2n}\right)^2\frac{r_0^2 f_0^2}{2f_e}\frac{\partial f_e}{\partial z}+\phi(z). \quad (25)$$

To solve the Eqs. (22), (24), and (25), we have used the boundary condition at $z=0, f_e=1$ & $\partial f_e/\partial z=0;$ and equating the power of η^2, one gets

$$\frac{\partial^2 f_e}{\partial \xi^2}=\frac{f_e\rho_0^2}{f_0^2}\left[\begin{array}{c}\frac{1}{k^2 r_0^2 f_0^2}\left\{3+\left(\frac{r_0 f_0}{af_e}\right)^4\right\}-2\frac{\omega_p^2}{\gamma k^2 v_{th}^2}\\ \times\left\{\frac{3}{4}\alpha\frac{m_e}{m_i}\frac{E_0^2}{f_0^2}\exp(-2n)n^{2n}\right\}\\ \exp\left\{-\frac{3}{4}\alpha\frac{m_e}{m_i}\frac{E_0^2}{f_0^2}\exp(-2n)n^{2n}\right\}\end{array}\right]. \quad (26)$$

Where, $k_i=\frac{\Gamma_e\omega}{kv_{th}^2}$ is the damping factor.

3. STIMULATED RAMAN SCATTERING

Consider the high frequency electric field E_T which is the sum of the electric field of scattered wave E_S and the electric field of pump laser beam E_i.

$$E_H=E_i e^{i\omega_0 t}+E_S e^{i\omega_s t} \quad (27)$$

Where, ω_0 and ω_S are the incident laser beam and scattered wave frequency, respectively. The wave equation for the scattered field can be written as

$$\nabla^2 E_s-\frac{\omega_s^2}{c^2}\left(1-\frac{\omega_p^2}{\omega_s^2}\frac{N_{0e}}{N_0}\right)E_s=\frac{\omega_p^2}{2c^2}\frac{\omega_s}{\omega_0}\frac{n^*}{N_0}E_i. \quad (28)$$

The solution of Eq. (28) can be written as

$$E_s=E_{s0}(r,z)e^{ik_{s0}z}+E_{s1}(r,z)e^{-ik_{s1}z}. \quad (29)$$

Where, $k_{s0}=\frac{\omega_s^2}{c^2}\varepsilon_s(0)$, k_{S1} and ω_S satisfy the phase matching condition.

$$k_{S1}=k_0-k,\ \omega_S=\omega_0-\omega. \quad (30)$$

From Eqs. (28) and (29), one gets

$$\left(\frac{1}{r}\frac{\partial E_{S0}}{\partial r}+\frac{\partial^2 E_{S0}}{\partial r^2}\right)+2ik_{S0}\frac{\partial E_{S0}}{\partial z}-k_{S0}^2 E_{S0}+\frac{\omega_S^2}{c^2}\in_S(r,z)E_{S0}=0, \quad (31)$$

$$\left(\frac{1}{r}\frac{\partial E_{S1}}{\partial r}+\frac{\partial^2 E_{S1}}{\partial r^2}\right)-2ik_{S1}\frac{\partial E_{S1}}{\partial z}-k_{S0}^2 E_{S1}+\frac{\omega_S^2}{c^2}\in_S(r,z)E_{S1}=\frac{1}{2}\frac{\omega_p^2}{c^2}\frac{\omega_S}{\omega_0}\frac{n^*}{N_0}E_0 e^{-ik_0 S_0}. \quad (32)$$

Where, $\varepsilon_S(r,z)=1-\frac{\omega_p^2}{\omega_S^2}\left(\frac{N_{0e}}{N_0}\right)$.

To simplify the Eq. (31), one can substitute $E_{S0}=E_{S00}(r,z)\,e^{ik_{s0}S_c}$ in Eq. (31) and separating the real and imaginary part, one can get

$$2\left(\frac{\partial S_c}{\partial z}\right)+\left(\frac{\partial S_c}{\partial r}\right)^2=\frac{1}{k_{s0}^2 E_{s00}}\left(\frac{\partial^2 E_{s00}}{\partial r^2}+\frac{1}{r}\frac{\partial E_{r00}}{\partial r}\right)+\frac{\omega_S^2}{k_{S0}^2 c^2}\left\{\in_S-\in_S(0)\right\}, \quad (33)$$

$$\frac{\partial E_{s00}^2}{\partial z}+E_{s00}^2\left(\frac{\partial^2 S_c}{\partial r^2}+\frac{1}{r}\frac{\partial S_c}{\partial r}\right)+\left(\frac{\partial E_{s00}^2}{\partial r}\right)\left(\frac{\partial S_c}{\partial r}\right)=0. \quad (34)$$

Now transform the (r,z) coordinate in to (η, z) coordinate by using the Eq. (9) and the solution of the Eqs. (33) and (34) can be written as

$$E_{s00}^2=\frac{B'^2}{2^{2n}f_s^2}\left(\sqrt{2n}+\eta\right)^{4n}\left(\frac{r_0 f_0}{bf_s}\right)^{4n}\exp\left\{-\frac{r_0^2 f_0^2}{b^2 f_s^2}\left(\sqrt{2n}+\eta\right)^2\right\}, \quad (35)$$

$$S_c=\frac{\left(\sqrt{2n}+\eta\right)^2}{2}\frac{r_0^2 f_0^2}{f_s}\frac{\partial f_s}{\partial z}+\phi_s(z). \quad (36)$$

For an initial plane wave front, we used the boundary conditions $f_S=1,\ \frac{\partial f_S}{\partial z}=0$ at $z=0$. Using Eqs. (35) and (36) in Eq. (33) and equating the coefficient of $\eta^{2,}$ one gets

$$\frac{d^2 f_s}{d\xi^2}=\frac{f_s\rho_0^2}{f_0^2}\left\{\frac{1}{k_{S0}^2 r_0^2 f_0^2}\left\{3+\left(\frac{r_0 f_0}{bf_s}\right)^4\right\}-\frac{\omega_s^2}{k_{s0}^2 c^2}\in_{S2}\right\}. \quad (37)$$

In the presence of ponderomotive nonlinearity the $\varepsilon_S(\eta, z)$

can be expressed as

$$\varepsilon_S(\eta, z) = \varepsilon_S(0) - \eta^2 \varepsilon_{S2}. \tag{38}$$

Where

$$\varepsilon_S(0) = 1 - \frac{\omega_p^2}{\omega_S^2}\left\{\exp\left(-\frac{3}{4}\alpha\frac{m_e}{m_i}\frac{E_0^2}{f_0^2}n^{2n}e^{-2n}\right)\right\}, \tag{39}$$

$$\varepsilon_{S2} = 2\frac{\omega_p^2}{\omega_S^2}\left\{\frac{3}{4}\alpha\frac{m_e}{m_i}\frac{E_0^2}{f_0^2}n^{2n}e^{-2n}\exp\left(-\frac{3}{4}\alpha\frac{m_e}{m_i}\frac{E_0^2}{f_0^2}n^{2n}e^{-2n}\right)\right\}. \tag{40}$$

The value of B' may be obtained on applying appropriate boundary conditions

$$E_S = E_{S0}(r, z)e^{ik_{S0}z} + E_{S1}(r, z)e^{-ik_{S1}z} = 0 \text{ at } z = z_c.$$

Where, $z_c = L - z$ and L is the interaction length. Here, z_c is chosen sufficiently large so that n_{e00} is nearly zero. Therefore, at $z = z_c$, one gets

$$B' = \frac{1}{2^{n+1}}\left(\frac{\omega_p^2}{c^2}\right)\left(\frac{n_0}{N_0}\right)\left(\frac{\omega_s}{\omega_0}\right)\frac{f_s(z_c)}{f_e(z_c)f_s(z_c)}\left(\frac{r}{af_e(z_c)}\right)^{2n} \times \left(\frac{r}{r_0f_0(z_c)}\right)^{2n}\left(\frac{bf_s(z_c)}{r}\right)^{2n} \frac{E_{00}e^{-ik_iz_c}}{\left\{k_{s1}^2 - k_{s0}^2 - \frac{\omega_p^2}{c^2}\left(1 - \frac{N_{0e}}{N_0}\right)\right\}}\frac{e^{-i(k_0S_0 + k_{s0}S_c)}}{e^{i(k_{s0}z_c + k_{S1}z_c)}}. \tag{41}$$

With the condition

$$\frac{1}{a^2f_e^2(z_c)} + \frac{1}{r_0^2f_0^2(z_c)} = \frac{1}{b^2f_s^2(z_c)}. \tag{42}$$

Back reflectivity is defined as the ratio of back scattered power to the incident power, and is given by

$$R \simeq \frac{1}{4}\left(\frac{\omega_p^2}{c^2}\right)^2\left(\frac{n_0}{N_0}\right)^2\left(\frac{\omega_s}{\omega_0}\right)^2\frac{1}{\left\{k_{s1}^2 - k_{s0}^2 - \frac{\omega_p^2}{c^2}\left(1 - \frac{N_{0e}}{N_0}\right)\right\}^2} \times \left(\frac{r_0f_0}{af_e}\right)^{4n}\frac{\left(\eta + \sqrt{2n}\right)^{8n}}{2^{4n}f_e^2f_0^2} \exp\left\{-\left(\eta + \sqrt{2n}\right)^2\frac{r_0^2f_0^2}{a^2f_e^2} - \left(\eta + \sqrt{2n}\right)^2 - 2k_iz\right\}. \tag{43}$$

4. RESULT AND DISCUSSION

In collisionless plasma, the density of the plasma varies due to the ponderomotive force and the refractive index increases at the position of maximum irradiance; and the laser gets focused in the plasmas. Eqs. (9) and (10) describe the intensity profile of HGBs in plasma along the radial direction in the presence of ponderomotive nonlinearity. The intensity profile of the laser beam depends on the beam width f_0 in the paraxial regime; and Eq. (12) determines the focusing/defocusing of laser beam along the distance of propagation in plasma. In Eq. (12), on the right-hand side, the first term is responsible for diffraction, while the second term is responsible for the converging behavior of the beam during propagation in plasma. Numerical evaluation of Eqs. (9) and (12) are performed by using the typical laser beam parameters: the vacuum wavelength of the laser beam ($\lambda = 1064$ nm), laser power flux (10^{18}W/cm^2), the initial radius of the laser beam $r_0 = 10$ μm, the initial radius of the EPW $a = 10$ μm, plasma density $n/n_{cr} = 0.2$ and electron thermal speed $v_{th} = 0.1c$. Eq. (12) has been solved for an initial plane wave front of the hollow Gaussian beam and the numerical

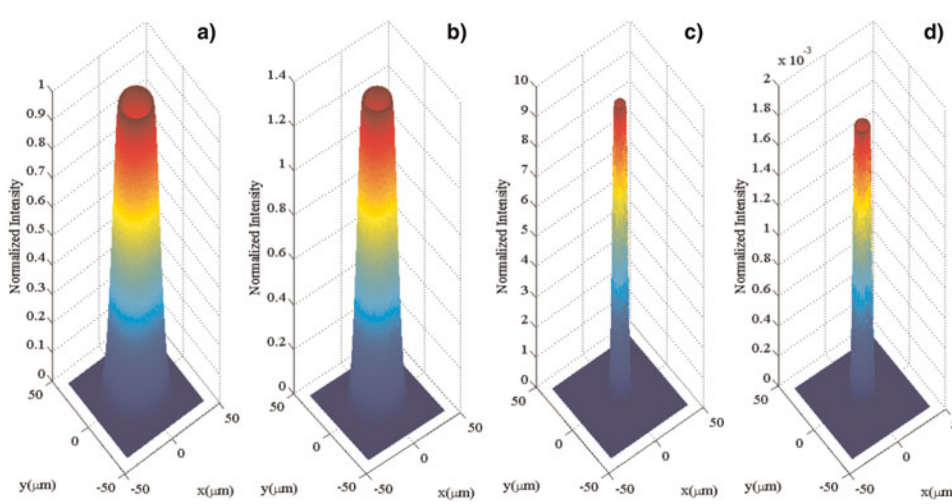

Fig. 1. (Color online) Normalized intensity distribution for order 1. (**a**) HGB and EPW at $\xi = 0$, (**b**) HGB at first focal point, (**c**) EPW at first focal point, (**d**) Back SRS at first focal point.

https://doi.org/10.1017/S0263034613000384 Published online by Cambridge University Press

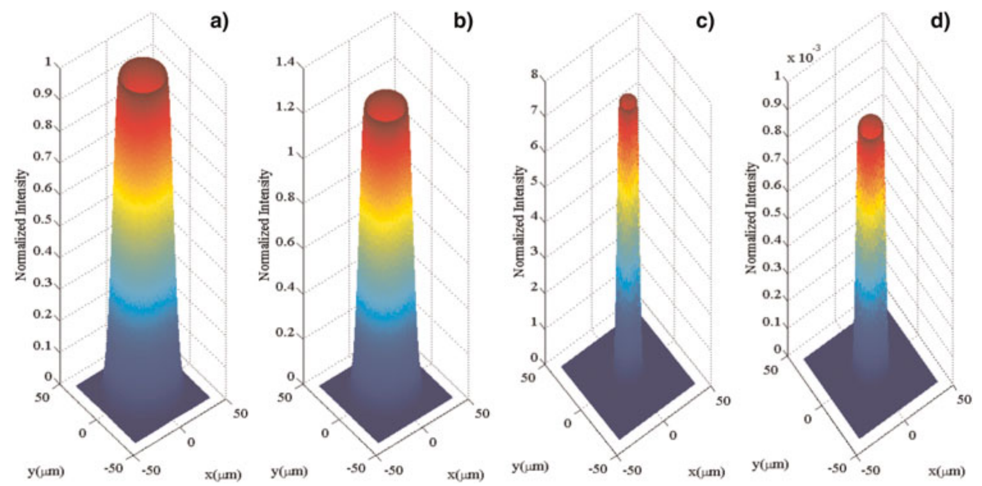

Fig. 2. (Color online) Normalized intensity distribution for order 2. (**a**) HGB and EPW at $\xi = 0$, (**b**) HGB at first focal point, (**c**) EPW at first focal point, (**d**) Back SRS at first focal point.

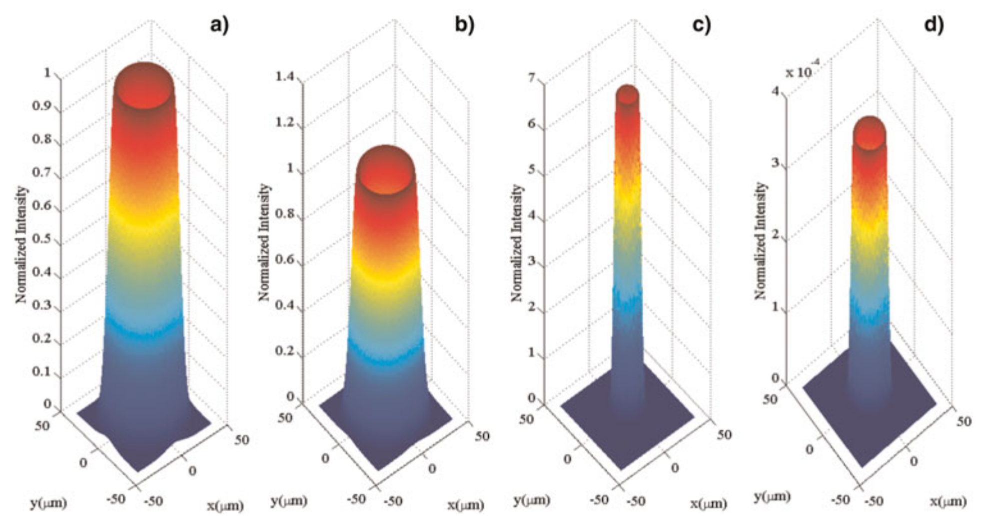

Fig. 3. (Color online) Normalized intensity distribution for order 3. (**a**) HGB and EPW at $\xi = 0$, (**b**) HGB at first focal point, (**c**) EPW at first focal point, (**d**) Back SRS at first focal point.

results are presented in the form of Figures 1, 2, and 3. The variation of intensity for the EPW on the order 1, 2, and 3 have been shown in Figures 1a, 2a, and 3a, respectively at $\xi = 0$; while in Figures 1b, 2b, and 3b at first focal point (beam focused position) with normalized distance ξ. It is obvious from the figure that in paraxial regime the intensity of laser beam is maximum at $\eta = 0$; and at first focal point the intensity of laser beam decreases with increase in the order of the HGBs.

When the high power HGBs propagates through plasma, the motion of electron will be modified due to ponderomotive nonlinearity and will give rise to change in the nonlinear current density. The density profile of plasma is modified and governed by the Eq. (24). The intensity profile of the EPW depends on the beam width parameter f_e in the paraxial regime. We have solved Eq. (26) numerically to obtain the amplitude of the density perturbation at finite z. The results are displayed in Figures 1a, 2a, and 3a, which show that the EPW gets excited due to nonlinear coupling with high power laser beam in the presence of ponderomotive nonlinearity and similar kind of result observed by Mendonca *et al.* (2009) without introducing the nonlinearity term. The EPW is also having the maximum intensity (for different order of HGBs) at $\eta = 0$ in the paraxial regime. Figures 1c, 2c, and 3c depicts that the variation in intensity for order 1, 2, and 3 of EPWs at first focal point, with normalized distance ξ, respectively.

Eq. (37) expresses the beam width parameter of the scattered beam and Eq. (43) gives the reflectivity against the distance of propagation. The result displayed in Figures 1d, 2d, and 3d shows the normalized intensity of the back reflected laser beam at the focal point for order 1, 2, and 3, respectively. We have solved Eq. (43) numerically and the results are presented in the form of Figure 4, which shows the

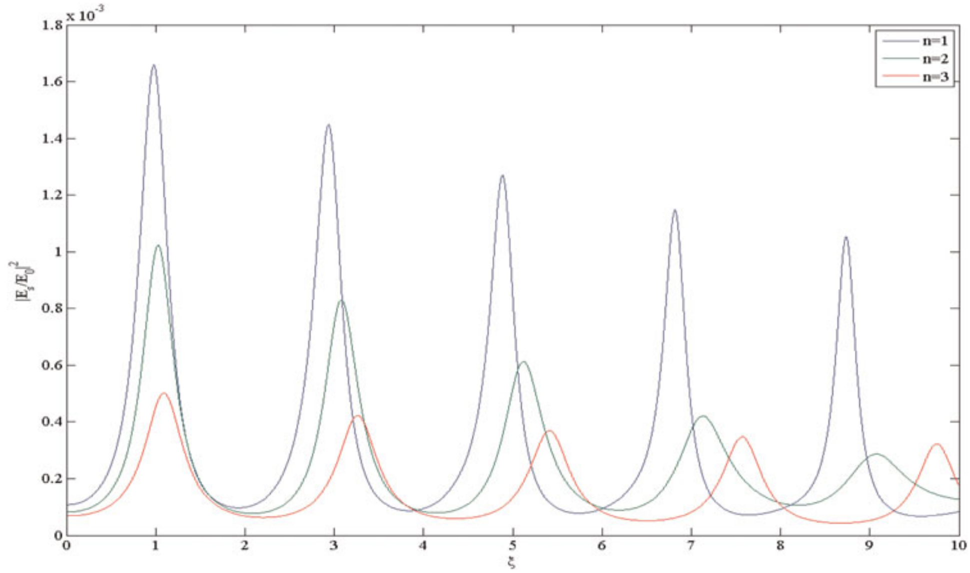

Fig. 4. (Color online) Variation of back reflectivity against normalized distance of propagation ξ.

variation of the back reflectivity with normalized distance for different order of HGBs around the maximum irradiance $\eta = 0$. In Figure 4, the back reflectivity for different order of HGBs are presented with normalized distance ξ and is maximum at the focal points of the focused laser beam. It is also shown that as we increase the order of the HGBs the reflectivity decreases because the focusing of HGBs decreases with increasing order of the beam.

5. CONCLUSION

For deeper understanding in laser plasma interaction, higher modes of laser beam are also important because the total field is superposition of all the modes in cylindrical coordinates. The earlier work in laser plasma interaction is limited to TEM_{00} mode which has maximum intensity at the center but in the presence of higher modes, intensity profile should be modified. In the present article, we studied the excitation of EPW in the presence of laser beam which has null intensity at the center. The focusing of the HGBs, excitation of EPW and back reflectivity of HGBs has been investigated. These results should find applications in the laser induced fusion scheme where higher modes are also present in the laser beam.

ACKNOWLEDGMENT

This work was partially supported by Department of Science and Technology (DST), India and University Grant Commission (UGC), India.

REFERENCES

Akhmanov, S.A., Sukhorukov, A.P. & Khokhlov, R.V. (1968). Self-focusing and diffraction of light in a nonlinear medium. *Sov. Phys. Usp.* **10**, 609–636.

Allen, L., Beijersbergen, M.W., Spreeuw, R.J.C. & Woerdman, J.P. (1992). Orbital angular momentum of light and the transformation of Laguerre-Gaussian laser modes. *Phys. Rev. A.* **45**, 8185–8189.

Cai, Y., Lu, X. & Lin, Q. (2003). Hollow Gaussian beam and their propagation properties. *Opt. Lett.* **28**, 1084–1086.

Cai, Y. & Zhang, L. (2006). Propagation of various dark hollow beams in a turbulent atmosphere. *Opt. Express* **14**, 1353–1367.

Cai, Y. & Lin, Q. (2004). Hollow elliptical Gaussian beam and its propagation through aligned and misaligned paraxial optical systems. *J. Opt. Soc. Am. A* **21**, 6.

Fuchs, J., Labaune, C., Depierreux, S., Tikhonchuk, V.T. & Baldis, H.A. (2000). Stimulated Brillouin and Raman scattering from a randomized laser beam in large inhomogeneous collisional plasmas. I. Experiment. *Phys. Plasmas* **7**, 4659–4668.

Grow, D.T., Ishaaya, A.A., Vuong, L.T. & Gaeta, A.L. (2006). Collapse dynamics of supper-Gaussian beam. *Opt. Soc. Am.* **14**, 5468.

Gupta, Ruchika., Sharma, Prerana., Rafat, M. & Sharma, R.P. (2011). Cross-focusing of two hollow Gaussian laser beam in plasma. *Laser Part. Beams* **29**, 227–230.

Gill, T.S., Mahajan, R. & Kaur, R. (2010). Relativistic and ponderomotive effects on evolution of dark hollow Gaussian electromagnetic beams in a plasma. *Laser Part. Beams* **28**, 521–529.

Herman, R.M. & Wiggins, T.A. (1991). Production and uses of diffractionless beams. *J. Opt. Soc. Am. A* **8**, 932.

Kaw, P.K., Schmidt, G. & Wilcox, T. (1973). Filamentation and trapping of electromagnetic radiation in plasma. *Phys. Fluids* **16**, 1522.

Kruer, W.L. (1974). *The Physics of Laser Plasma Interaction*. New York: Addison-Wesley.

Kirkwood, R.K., Moody, J.D., Niemann, C., Williams, E.A., Langdon, A.B., Landen, O.L., Divol, L. & Suter, L.J. (2006). Observation of polarization dependent Raman scattering in a large scale plasma illuminated with multiple laser beam. *Phys. Plasmas* **13**, 082703.

Lee, H.S., Stewart, B.W., Choi, K. & Fenichel, H. (1994). Holographic nondiverging hollow beam. *Phys. Rev. A* **49**, 4922.

Michelberg, H.M., Durfee, C.G. III & Mcilarth, T.J. (1995). High-order frequency conversion in the plasma waveguide. *Phys. Rev. Lett.* **75**, 2494–2497.

Mendonca, J.T., Thide, B. & Then, H. (2009). Stimulated Raman and Brillouin backscattering of collimated beams carrying orbital angular momentum. *Phys. Rev. Lett.* **102**, 185005.

Matsuoka, T., Lei, A., Yabuuchi, T., Adumi, K., Zheng, J., Kodamal, R., Sawai, K., Suzuki, K., Kitagawa, Y., Norimatsu, T., Nagai, K., Nagatomo, H., Izawa, Y., Mima, K., Sentoku, Y. & Tanaka, K.A. (2008). Focus optimization of relativistic self-focusing for anomalous laser penetration into overdense plasmas (super- penetration). *Plasma Phys. Control. Fusion* **50**, 10501.

Sodha, M.S., Misra, S.K. & Misra, S. (2009). Focusing of dark hollow Gaussian electromagnetic beams in a plasma. *Laser Part. Beams* **27**, 57–68.

Sodha, M.S., Ghatak, A.K. & Tripathi, V.K. (1976). Self focusing of laser beams in plasmas and semiconductors. *Prog. Opt. E* **3**, 169–265.

Sprangle, P. & Esarey, E. (1991). Stimulated backscattered harmonic generation from intense laser interactions with beams and plasmas. *Phys. Rev. Lett.* **67**, 2021–2024.

Sprangle, P., Esarey, E., Ting, A. & Joyce, G. (1988). Laser wakefield acceleration and relativistic optical guiding. *Appl. Phys. Lett.* **53**, 2146–2148.

Song, Y., Milam, D. & Hill, W.T. (1999). Long, narrow all-light atom guide. *Opt. Lett.* **24**, 1805.

Tabak, M., Hammer, J., Glinisky, M.E., Kruer, W.L., Wilks, S.C., Woodworth, J., Campbell, E.M., Perry, M.D. & Mason, R.J. (1994). Ignition and high gain with ultra powerful lasers. *Phys. Plasmas* **1**, 1626–1634.

Tajima, T. & Dawson, J.M. (1979). Laser electron accelerator. *Phys. Rev. Lett.* **43**, 267.

Umstadter, D., Chen, S.Y., Maksimchuk, A., Mourou, G. & Wagner, R. (1996). Nonlinear optics in relativistic plasmas and laser wakefield acceleration of electrons. *Sci.* **273**, 472–475.

Umstadter, D., Kim, J.K. & Dodd, E. (1996). Laser injection of ultrashort electron pulses into wakefield plasma waves. *Phys. Rev. Lett.* **76**, 2073.

Umstadter, D. & Norris, T.B. (1997). Nonlinear optics with relativistic electrons. *IEEE J. Quantum Electr.* **33**, 1877.

Wang, X. & Littman, M.G. (1993). Laser cavity for generation of variable-radius rings of light. *Opt. Lett.* **18**, 767.